

Detrended Partial Cross-correlation Analysis of Two Time Series Influenced by Common External Forces

Xi-Yuan Qian,^{1,2} Ya-Min Liu,¹ Zhi-Qiang Jiang,^{2,3} Boris Podobnik,^{4,5,6} Wei-Xing Zhou,^{1,2,3,*} and H. Eugene Stanley^{4,†}

¹*School of Science, East China University of Science and Technology, Shanghai 200237, China*

²*Research Center for Econophysics, East China University of Science and Technology, Shanghai 200237, China*

³*School of Business, East China University of Science and Technology, Shanghai 200237, China*

⁴*Center for Polymer Studies and Department of Physics, Boston University, Boston, MA 02215, USA*

⁵*Faculty of Civil Engineering, University of Rijeka, 51000 Rijeka, Croatia*

⁶*Zagreb School of Economics and Management, 10000 Zagreb, Croatia*

(Dated: December 3, 2024)

We propose a new method, detrended partial cross-correlation analysis (DPXA), to uncover the intrinsic power-law cross-correlations between two simultaneously recorded time series in the presence of nonstationarity after removing the effects of other time series acting as common forces. The DPXA method is a generalization of the detrended cross-correlation analysis by taking into account the partial correlation analysis. We illustrate the performance of the method using bivariate fractional Brownian motions and multifractal binomial measures with analytical expressions and apply it to extract the intrinsic cross-correlation between crude oil and gold futures by considering the impact of the US dollar index.

PACS numbers: 89.75.Da, 05.45.Tp, 05.45.Df, 05.40.-a

Complex systems with interacting constituents are ubiquitous in nature and society. To understand the microscopic mechanisms of emerging statistical laws of complex systems, one records and analyzes time series of observable quantities. These time series are usually nonstationary and possess long-range power-law cross-correlations. Examples include the velocity, temperature, and concentration fields of turbulent flows embedded in the same space as joint multifractal measures [1, 2], topographic indices and crop yield in agronomy [3, 4], temporal and spatial seismic data [5], nitrogen dioxide and ground-level ozone [6], heart rate variability and brain activity of healthy humans [7], wind patterns and land surface air temperature [8], traffic flows [9], self-affine time series of taxi accidents [10], econophysical variables [11–13], and so on. Methods such as detrended cross-correlation analysis were invented to investigate the long-range power-law cross-correlations between two nonstationary time series [14–20].

However, it is very likely that the observed long-range power-law cross-correlations between two time series do not reflect their intrinsic relationship but are caused by a common third driving force [21–23]. If the influence of the common driving force on the two time series are additive, we can adopt the notion of partial correlation to unveil their intrinsic relationship [24]. To extract the intrinsic long-range power-law cross-correlations between two time series conditional on a third driving force, we propose in this Letter a class of methods which we call detrended partial cross-correlation analysis (DPXA), where we combine the ideas of detrended cross-correlation analysis and partial correlation.

Consider two stationary time series $\{x(t) : t =$

$1, \dots, T\}$ and $\{y(t) : t = 1, \dots, T\}$, which depend on a sequence of time series $\{z_i(t) : t = 1, 2, \dots, T\}$ with $i = 1, \dots, n$. Each time series is covered with $M_s = [T/s]$ non-overlapping windows of size s . Consider the v th box $[l_v + 1, l_v + s]$, where $l_v = (v - 1)s$. We calibrate the two linear regression models for \mathbf{x}_v and \mathbf{y}_v respectively:

$$\begin{cases} \mathbf{x}_v = \mathbf{Z}_v \boldsymbol{\beta}_{x,v} + \mathbf{r}_{x,v} \\ \mathbf{y}_v = \mathbf{Z}_v \boldsymbol{\beta}_{y,v} + \mathbf{r}_{y,v} \end{cases}, \quad (1)$$

where $\mathbf{x}_v = [x_{l_v+1}, \dots, x_{l_v+s}]^T$, $\mathbf{y}_v = [y_{l_v+1}, \dots, y_{l_v+s}]^T$, $\mathbf{r}_{x,v}$ and $\mathbf{r}_{y,v}$ are the vectors of error term, and

$$\mathbf{Z}_v = \begin{pmatrix} \mathbf{z}_{v,1}^T \\ \vdots \\ \mathbf{z}_{v,p}^T \end{pmatrix} = \begin{pmatrix} \mathbf{z}_1(l_v + 1) & \cdots & \mathbf{z}_p(l_v + 1) \\ \vdots & \ddots & \vdots \\ \mathbf{z}_1(l_v + s) & \cdots & \mathbf{z}_p(l_v + s) \end{pmatrix} \quad (2)$$

is the matrix of the p external forces in the v th box, where \mathbf{x}^T is the transform of \mathbf{x} . Equation (1) gives the estimates $\hat{\boldsymbol{\beta}}_{x,v}$ and $\hat{\boldsymbol{\beta}}_{y,v}$ of the p -dimensional parameter vectors $\boldsymbol{\beta}_{x,v}$ and $\boldsymbol{\beta}_{y,v}$ and the sequences of error terms:

$$\begin{cases} \mathbf{r}_{x,v} = \mathbf{x}_v - \mathbf{Z}_v \hat{\boldsymbol{\beta}}_{x,v} \\ \mathbf{r}_{y,v} = \mathbf{y}_v - \mathbf{Z}_v \hat{\boldsymbol{\beta}}_{y,v} \end{cases}. \quad (3)$$

The profiles of the disturbances are obtained as follow

$$\begin{cases} R_{x,v}(k) = \sum_{j=1}^k r_x(l_v + j) \\ R_{y,v}(k) = \sum_{j=1}^k r_y(l_v + j) \end{cases}, \quad (4)$$

where $k = 1, \dots, s$.

Assume that the local trend functions of $R_{x,v}$ and $R_{y,v}$ are $\tilde{R}_{x,v}$ and $\tilde{R}_{y,v}$, respectively. The detrended partial

cross-correlation in each window we calculate as follows:

$$F_v^2(s) = \frac{1}{s} \sum_{k=1}^s [R_{x,v}(k) - \tilde{R}_{x,v}(k)] [R_{y,v}(k) - \tilde{R}_{y,v}(k)] \quad (5)$$

The second-order detrended partial cross-correlation is calculated as follows:

$$F_{xy:z}(2, s) = \left[\frac{1}{m-1} \sum_{v=1}^m F_v^2(s) \right]^{1/2}. \quad (6)$$

If there exist intrinsic long-range power-law cross-correlations between x and y , we expect the following scaling relation

$$F_{xy:z}(2, s) \sim s^{h_{xy:z}}. \quad (7)$$

There are many different methods for the determination of $\tilde{R}_{x,v}$ and $\tilde{R}_{y,v}$. The local detrending functions could be polynomials [25, 26], moving averages [27–30], and other alternates [31]. To distinguish different detrending methods, we can term the corresponding DPXA variants as PX-DFA, PX-DMA, and so on. When the moving average is used as the local detrending function, the window size of the moving averages should be the same as the covering window size s [32].

In order to investigate the validity and performance of the DPXA method, we perform extensive numerical experiments based on the following additive model for x and y :

$$\begin{cases} x(t) = \beta_{x,0} + \beta_x z(t) + r_x(t) \\ y(t) = \beta_{y,0} + \beta_y z(t) + r_y(t) \end{cases}, \quad (8)$$

where $z(t)$ is a fractional Gaussian noise with Hurst index H_z , while r_x and r_y are the increment series of the two components of a bivariate fractional Brownian motions (BFBMs) with Hurst indexes H_{r_x} and H_{r_y} [33–35]. The basic properties of multivariate fractional Brownian motions have been extensively studied [33–35]. Particularly, it has been proven that the Hurst index $H_{r_x r_y}$ of the cross-correlation between the two components is [33–35]:

$$H_{r_x r_y} = (H_{r_x} + H_{r_y})/2. \quad (9)$$

This property allows us to investigate the performances of the proposed methods on a solid foundation. Specifically, we can obtain h_{xy} of x and y using the DCCA method and $h_{xy:z}$ of r_x and r_y using the DPXA method. Our numerical experiments show that $H_{r_x r_y} = h_{r_x r_y} = h_{xy:z} \neq h_{xy}$. In this Letter, we use H for theoretical or true values and h for numerical estimates.

In the simulations, we set $\beta_{x,0} = 2$, $\beta_x = 3$, $\beta_{y,0} = 2$, and $\beta_y = 3$ in the model of Eq. (8). Three Hurst indexes H_{r_x} , H_{r_y} and H_z are input arguments, varying from 0.1 to 0.95 with a spacing of 0.05. Because

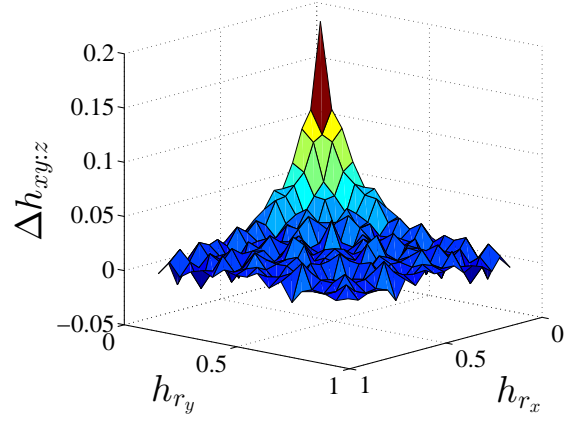


FIG. 1. (color online.) Relative error $\Delta h_{xy:z}$ between the DPXA estimate $\langle h_{xy:z} \rangle_z$ and the true value $h_{r_x r_y}$ as a function of h_{r_x} and h_{r_y} .

r_x and r_y are symmetric, we set $H_{r_x} \leq H_{r_y}$, resulting in $\frac{(18+1) \times 18}{2} \times 18 = 3078$ triplets of (H_{r_x}, H_{r_y}, H_z) . The BFBMs are simulated using the method provided in Ref. [34, 35], while the FBM are generated with a fast wavelet-based approach [36]. Each time series has length of 65536. For each (H_{r_x}, H_{r_y}, H_z) triplet, we conduct 100 repeated simulations. We obtain the Hurst indexes for the simulated time series r_x , r_y , z , x and y using the detrended fluctuation analysis [25, 37], and the average values h_{r_x} , h_{r_y} , h_z , h_x , and h_y over 100 realizations are calculated for further analysis. Linear regression between the output and input Hurst indexes gives that $\langle h_{r_x} \rangle = 0.009 + 0.990 H_{r_x}$, $\langle h_{r_y} \rangle = 0.009 + 0.990 H_{r_y}$, and $\langle h_z \rangle = 0.010 + 0.991 H_z$, suggesting that the generated FBM have the desired Hurst indexes equal to the input Hurst indexes (see Supplemental Material [38]). When h_{r_x} is less than or close to h_z , h_x is found to be close to h_z ; Otherwise, $h_z < h_x < h_{r_x}$ (see Supplemental Material [38]).

We find that $h_{r_x r_y} = (h_{r_x} + h_{r_y})/2$ (we show a plot in Supplemental Material [38]). Because $h_{r_x} \approx H_{r_x}$ and $h_{r_y} \approx H_{r_y}$ (see Supplemental Material [38]), we have $h_{r_x r_y} \approx H_{r_x r_y}$. We also find that $h_{xy} \approx (h_x + h_y)/2$ (we show a plot in Supplemental Material [38]). We note that $h_{xy:z}$ is a function of h_{r_x} , h_{r_y} and h_z . A simple linear regression gives

$$h_{xy:z} = 0.003 + 0.509 h_{r_x} + 0.493 h_{r_y} + 0.012 h_z, \quad (10)$$

which illustrates that the DPXA method is able to extract excellently the intrinsic cross-correlations between the two time series x and y influenced by a common factor z . We calculate the average $\langle h_{xy:z} \rangle_z$ over different H_z , and then obtain the following relative error:

$$\Delta h_{xy:z} = \frac{\langle h_{xy:z} \rangle_z - h_{r_x r_y}}{h_{r_x r_y}}. \quad (11)$$

The results for different combinations of h_{r_x} and h_{r_y} are

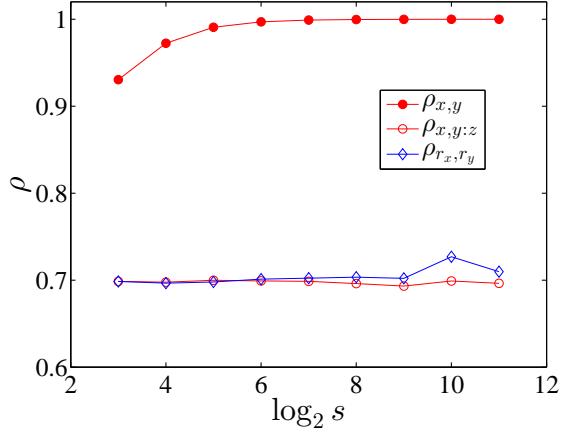


FIG. 2. (color online.) Performance of different methods by comparing three cross-correlation coefficients $\rho_{x,y}$, ρ_{r_x, r_y} and $\rho_{x,y,z}$ of the mathematical model in Eq. (8).

illustrated in Fig. 1. For most combinations, we observe that $\Delta h_{xy,z} \ll 0.05$. However, when both h_{r_x} and h_{r_y} approach 0, $\Delta h_{xy,z}$ becomes large. When $h_{r_x} = h_{r_y} = 0.11$, $\Delta h_{xy,z} = 0.192$, while when $h_{r_x} = 0.11$ and $h_{r_y} = 0.16$, $\Delta h_{xy,z} = 0.113$. For all other points of (h_{r_x}, h_{r_y}) , the relative errors $\Delta h_{xy,z}$ are less than 0.10.

Similar to the detrended cross-correlation coefficients [39, 40], we can define the detrended partial cross-correlation coefficient (or DPXA coefficient) as follows:

$$\rho_{\text{DPXA}}(s) = \rho_{xy,z}(s) = \frac{F_{xy,z}^2(2, s)}{F_{x,z}(2, s)F_{y,z}(2, s)}. \quad (12)$$

As for the DCCA coefficient [40, 41], for DPXA we also have $-1 \leq \rho_{\text{DPXA}}(s) \leq 1$. The DPXA coefficient is expected to measure the intrinsic cross-correlations between two non-stationary series.

We first show the effectiveness of the DPXA coefficient and its out-performance over the DCCA coefficient using the mathematical model in Eq. (8) with the coefficients $\beta_{x,0} = \beta_{y,0} = 2$ and $\beta_{x,1} = \beta_{y,1} = 3$. The two components r_x and r_y of the BFBM have very small Hurst indexes $H_{r_x} = 0.1 = H_{r_y} = 0.1$ and their correlation coefficient is $\rho = 0.7$, while the driving FBM force z has a large Hurst index $H_z = 0.95$. The resulting cross-correlation coefficients at different scales are illustrated in Fig. 2. The DCCA coefficients ρ_{r_x, r_y} between the generated r_x and r_y time series overestimate the true value $\rho = 0.7$. Because the influence of z on r_x and r_y is very strong, the behaviors of x and y are dominated by z so that the cross-correlation coefficient $\rho_{x,y}(s)$ is close to 1 when s is not too large and approaches to 1 for large s . In contrast, the DPXA coefficients $\rho_{x,y,z}(s)$ agree excellently with the true value $\rho = 0.7$. More intriguingly, the DPXA method gives better estimates than the DCCA method on r_x and r_y , since the ρ_{r_x, r_y} curve deviates more from the horizontal line $\rho = 0.7$ than the $\rho_{x,y,z}$

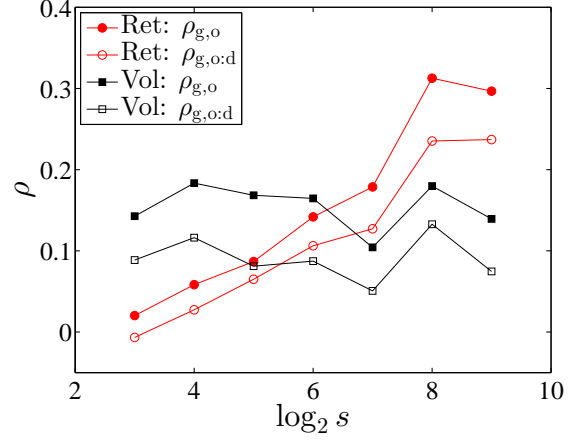


FIG. 3. (color online.) Estimation and comparison of the cross-correlation levels between the two return time series (\circ) and two volatility time series (\square) of crude oil and gold when including and excluding the influence of the USD index.

curve, especially at large scales.

Next we illustrate the method by selected example from finance. We apply the method to estimate the intrinsic cross-correlation levels between the futures returns and volatilities of crude oil and gold. It is well documented that the returns of crude oil futures and gold futures are correlated [42], and both commodities are influenced by the USD index [43]. The data samples contain the daily close prices of gold, crude oil and USD index from October 4, 1985 to October 31, 2012. Figure 3 shows that both the DCCA and DPXA coefficients of returns exhibit an increasing trend with respect to the scale s , while the two types of coefficient for the volatilities do not exhibit an evident trend. For both financial variables, we find that (See Fig. 2)

$$\rho_{g,o;d}(s) < \rho_{g,o}(s) \quad (13)$$

for different scales, which is reminiscent of the similar result between ordinary partial correlations and cross-correlations [44]. However, the DPXA coefficients contain more information than the ordinary partial correlations since the former unveil the partial correlations at multiple scales.

An extension of the DPXA for multifractal time series can be easily implemented, abbreviated as MF-DPXA. If the MF-DPXA is implemented with DFA or DMA, then it is called MF-PX-DFA or MF-PX-DMA. The q th order detrended partial cross-correlation is calculated as follows:

$$F_{xy,z}(q, s) = \left[\frac{1}{m} \sum_{v=1}^m |F_v^2(s)|^{q/2} \right]^{1/q} \quad (14)$$

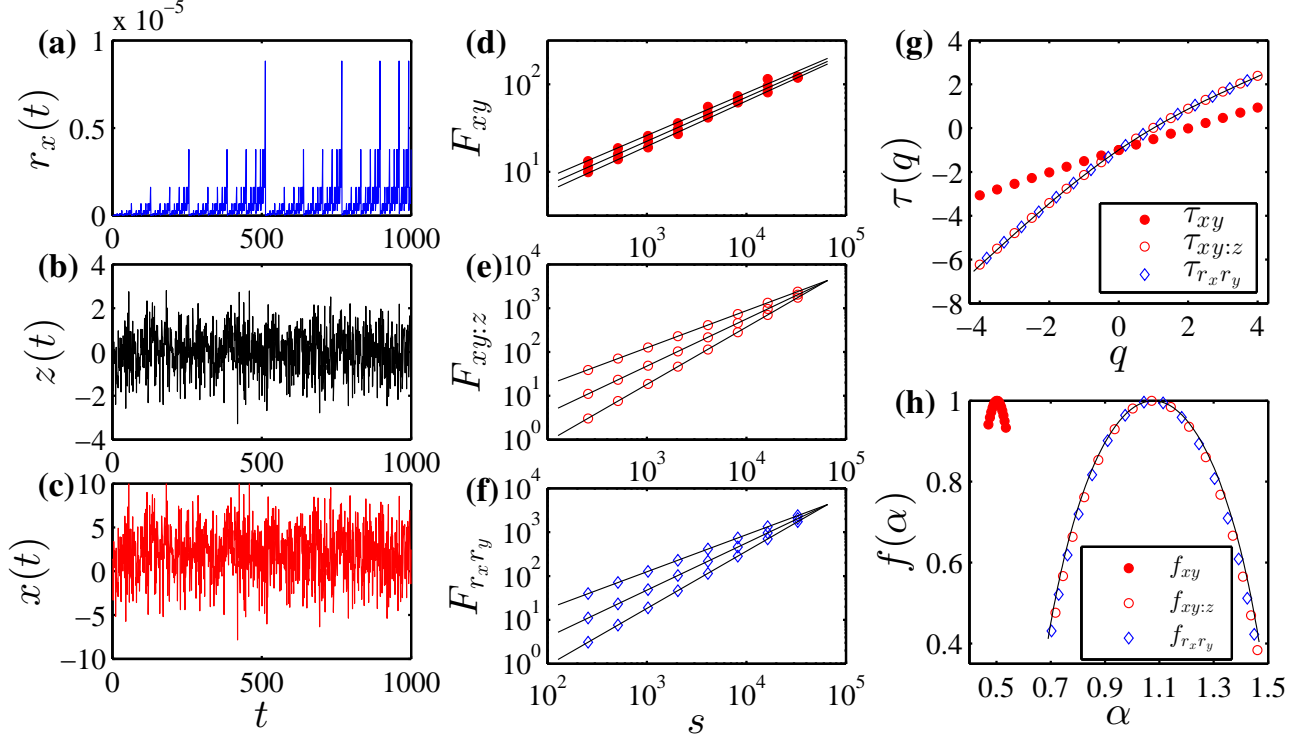


FIG. 4. (color online.) Multifractal detrended partial cross-correlation analysis of two binomial measures contaminated by Gaussian noise with very low signal-to-noise ratio. (a-c) The segments of the binomial signal $r_x(t)$ with $p_x = 0.3$, the Gaussian noise $z(t)$, and the “observed” signal $x(t)$. (d-f) Power-law dependence of the fluctuations $F_{xy}(q, s)$, $F_{xy:z}(q, s)$, $F_{r_x r_y}(q, s)$ on the scale s for $q = -4, 0$ and 4 (top down). The values of $F_{xy:z}$ and $F_{r_x r_y}$ have been multiplied by 10^5 . (g) Multifractal mass exponents $\tau_{xy}(q)$, $\tau_{xy:z}(q)$ and $\tau_{r_x r_y}(q)$, with the theoretical curve $\mathcal{T}_{r_x r_y}$ shown as a continuous line. (h) Multifractal spectra $f_{xy}(\alpha)$, $f_{xy:z}(\alpha)$, $f_{r_x r_y}(\alpha)$ of the singularity strength α . The continuous curve is the theoretical spectrum $\mathcal{F}_{r_x r_y}(\alpha)$.

when $q \neq 0$, and

$$F_{xy:z}(0, s) = \exp \left[\frac{1}{m} \sum_{v=1}^m \ln |F_v(s)| \right]. \quad (15)$$

We then expect the following scaling relation

$$F_{xy:z}(q, s) \sim s^{h_{xy:z}(q)}. \quad (16)$$

According to the standard multifractal formalism, the multifractal mass exponent $\tau(q)$ can be used to characterize the multifractal nature, which reads

$$\tau_{xy:z}(q) = q h_{xy:z}(q) - D_f, \quad (17)$$

where D_f is the fractal dimension of the geometric support of the multifractal measure [45]. For time series analysis, we have $D_f = 1$. If the mass exponent $\tau(q)$ is a nonlinear function of q , the signal has a multifractal nature. It is easy to obtain the singularity strength function $\alpha(q)$ and the multifractal spectrum $f(\alpha)$ via the Legendre transform [46]

$$\begin{cases} \alpha_{xy:z}(q) = d\tau_{xy:z}(q)/dq \\ f_{xy:z}(q) = q\alpha_{xy:z}(q) - \tau_{xy:z}(q) \end{cases}. \quad (18)$$

To test the performance of MF-DPXA, we construct two binomial measures $\{r_x(t) : t = 1, 2, \dots, 2^k\}$ and $\{r_y(t) : t = 1, 2, \dots, 2^k\}$ from the p -model with known analytic multifractal properties [47], and contaminate them with a Gaussian noise. The binomial measure are generated in an iterative way [19], and we use the multiplicative factors $p_x = 0.3$ for r_x and $p_y = 0.4$ for r_y . The contaminated signals are $x = 2 + 3z + r_x$ and $y = 2 + 3z + r_y$. As shown in Fig. 4(a-c), the signal-to-noise ratio is of order $O(10^{-6})$. Figures 4(d-f) show a nice power-law dependence of the fluctuation functions on the scale, in which it is hard to distinguish the three curves of F_{xy} . For $x(t)$ and $y(t)$, the $\tau_{xy}(q)$ function is almost a straight line in Fig. 4(g) and the corresponding $f_{xy}(\alpha)$ spectrum is very narrow and concentrated around $\alpha = 0.5$ in Fig. 4(h). These observations are trivial because $x(t)$ and $y(t)$ are Gaussian noise with the Hurst indexes $H_x = H_y = 0.5$ and the multifractal detrended cross-correlation analysis [16] fails to uncover any multifractality. On the contrary, we find that $\tau_{xy:z}(q) \approx \tau_{r_x r_y}(q) \approx \mathcal{T}_{r_x r_y}(q)$ and $f_{xy:z}(\alpha) \approx f_{r_x r_y}(\alpha) \approx \mathcal{F}_{r_x r_y}(\alpha)$, so that the MF-DPXA method successfully uncover the intrinsic multifractal nature between $r_x(t)$ and $r_y(t)$ hidden in $x(t)$ and $y(t)$.

The methods discussed so far are mainly intended for time series analysis, which can be easily generalized to high dimensions [19, 32, 48, 49]. We can also use lagged cross-correlations in these methods [50, 51]. Comparing the performance of different methods is always of significance importance [52]. However, different variants of a method may have different performance when applied to different systems.

This work was partially supported by National Natural Science Foundation of China under grant no. 11375064, Fundamental Research Funds for the Central Universities, and Shanghai Financial and Securities Professional Committee.

* wxzhou@ecust.edu.cn

† hes@bu.edu

- [1] R. A. Antonia and C. W. Van Atta, *J. Fluid Mech.* **67**, 273 (1975).
- [2] C. Meneveau, K. R. Sreenivasan, P. Kailasnath, and M. S. Fan, *Phys. Rev. A* **41**, 894 (1990).
- [3] A. N. Kravchenko, D. G. Bullock, and C. W. Boast, *Agron. J.* **92**, 1279 (2000).
- [4] T. B. Zeleke and B.-C. Si, *Agron. J.* **96**, 1082 (2004).
- [5] S. Shadkhoo and G. R. Jafari, *Eur. Phys. J. B* **72**, 679 (2009).
- [6] F. J. Jiménez-Hornero, J. E. Jiménez-Hornero, E. G. de Ravé, and P. Pavon-Domínguez, *Environ. Monit. Assess.* **167**, 675 (2010).
- [7] D.-C. Lin and A. Sharif, *Chaos* **20**, 023121 (2010).
- [8] F. J. Jiménez-Hornero, P. Pavón-Domínguez, E. G. de Rave, and A. B. Ariza-Villaverde, *Atoms. Res.* **99**, 366 (2011).
- [9] N. Xu, P.-J. Shang, and S. Kamae, *Nonlin. Dyn.* **61**, 207 (2010).
- [10] G. F. Zebende, P. A. da Silva, and A. M. Filho, *Physica A* **390**, 1677 (2011).
- [11] B. Podobnik, D. Horvatic, A. M. Petersen, and H. E. Stanley, *Proc. Natl. Acad. Sci. U.S.A.* **106**, 22079 (2009).
- [12] Y.-D. Wang, Y. Wei, and C.-F. Wu, *Physica A* **389**, 5468 (2010).
- [13] L.-Y. He and S.-P. Chen, *Chaos, Solitons & Fractals* **44**, 355 (2011).
- [14] W. C. Jun, G. Oh, and S. Kim, *Phys. Rev. E* **73**, 066128 (2006).
- [15] B. Podobnik and H. E. Stanley, *Phys. Rev. Lett.* **100**, 084102 (2008).
- [16] W.-X. Zhou, *Phys. Rev. E* **77**, 066211 (2008).
- [17] S. Arianos and A. Carbone, *J. Stat. Mech.*, P03037 (2009).
- [18] D. Horvatic, H. E. Stanley, and B. Podobnik, *EPL (Europhys. Lett.)* **94**, 18007 (2011).
- [19] Z.-Q. Jiang and W.-X. Zhou, *Phys. Rev. E* **84**, 016106 (2011).
- [20] L. Kristoufek, *EPL (Europhys. Lett.)* **95**, 68001 (2011).
- [21] D. Y. Kenett, Y. Shapira, and E. Ben-Jacob, *J. Prob. Stat.* **2009**, 249370 (2009).
- [22] Y. Shapira, D. Kenett, and E. Ben-Jacob, *Eur. Phys. J. B* **72**, 657 (2009).
- [23] D. Y. Kenett, M. Tumminello, A. Madi, G. Gershgoren, R. N. Mantegna, and E. Ben-Jacob, *PLoS One* **5**, e15032 (2010).
- [24] K. Baba, R. Shibata, and M. Sibuya, *Aust. N. Z. J. Stat.* **46**, 657 (2004).
- [25] C.-K. Peng, S. V. Buldyrev, S. Havlin, M. Simons, H. E. Stanley, and A. L. Goldberger, *Phys. Rev. E* **49**, 1685 (1994).
- [26] K. Hu, P. C. Ivanov, Z. Chen, P. Carpena, and H. E. Stanley, *Phys. Rev. E* **64**, 011114 (2001).
- [27] N. Vandewalle and M. Ausloos, *Phys. Rev. E* **58**, 6832 (1998).
- [28] E. Alessio, A. Carbone, G. Castelli, and V. Frappietro, *Eur. Phys. J. B* **27**, 197 (2002).
- [29] L. M. Xu, P. C. Ivanov, K. Hu, Z. Chen, A. Carbone, and H. E. Stanley, *Phys. Rev. E* **71**, 051101 (2005).
- [30] S. Arianos and A. Carbone, *Physica A* **382**, 9 (2007).
- [31] X.-Y. Qian, G.-F. Gu, and W.-X. Zhou, *Physica A* **390**, 4388 (2011).
- [32] G.-F. Gu and W.-X. Zhou, *Phys. Rev. E* **82**, 011136 (2010).
- [33] F. Lavancier, A. Philippe, and D. Surgailis, *Statist. Prob. Lett.* **79**, 2415 (2009).
- [34] J.-F. Coeurjolly, P.-O. Amblard, and S. Achard, *Eur. Signal Process. Conf.* **18**, 1567 (2010).
- [35] P.-O. Amblard, J.-F. Coeurjolly, F. Lavancier, and A. Philippe, *Bulletin Soc. Math. France, Séminaires et Congrès* **28**, 65 (2013).
- [36] P. Abry and F. Sellan, *Appl. Comp. Harmonic Anal.* **3**, 377 (1996).
- [37] J. W. Kantelhardt, E. Koscielny-Bunde, H. H. A. Rego, S. Havlin, and A. Bunde, *Physica A* **295**, 441 (2001).
- [38] See Supplemental Material at <http://link.aps.org/supplemental/10.1103/PhysRevLett.113.000000> for additional information on the ...
- [39] G. F. Zebende, *Physica A* **390**, 614 (2011).
- [40] L. Kristoufek, *Physica A* **406**, 169 (2014).
- [41] B. Podobnik, Z.-Q. Jiang, W.-X. Zhou, and H. E. Stanley, *Phys. Rev. E* **84**, 066118 (2011).
- [42] Y.-J. Zhang and Y.-M. Wei, *Resources Policy* **35**, 168 (2010).
- [43] Y. S. Wang and Y. L. Chueh, *Econometrica* **30**, 792 (2013).
- [44] D. Y. Kenett, X.-Q. Huang, I. Vodenska, S. Havlin, and H. E. Stanley, *Quant. Finance* **15**, 569 (2015).
- [45] J. W. Kantelhardt, S. A. Zschiegner, E. Koscielny-Bunde, S. Havlin, A. Bunde, and H. E. Stanley, *Physica A* **316**, 87 (2002).
- [46] T. C. Halsey, M. H. Jensen, L. P. Kadanoff, I. Procaccia, and B. I. Shraiman, *Phys. Rev. A* **33**, 1141 (1986).
- [47] C. Meneveau and K. R. Sreenivasan, *Phys. Rev. Lett.* **59**, 1424 (1987).
- [48] G.-F. Gu and W.-X. Zhou, *Phys. Rev. E* **74**, 061104 (2006).
- [49] A. Carbone, *Phys. Rev. E* **76**, 056703 (2007).
- [50] B. Podobnik, D. Wang, D. Horvatic, I. Grosse, and H. E. Stanley, *EPL (Europhys. Lett.)* **90**, 68001 (2010).
- [51] C.-H. Shen, *Phys. Lett. A* **379**, 680 (2015).
- [52] Y.-H. Shao, G.-F. Gu, Z.-Q. Jiang, W.-X. Zhou, and D. Sornette, *Sci. Rep.* **2**, 835 (2012).

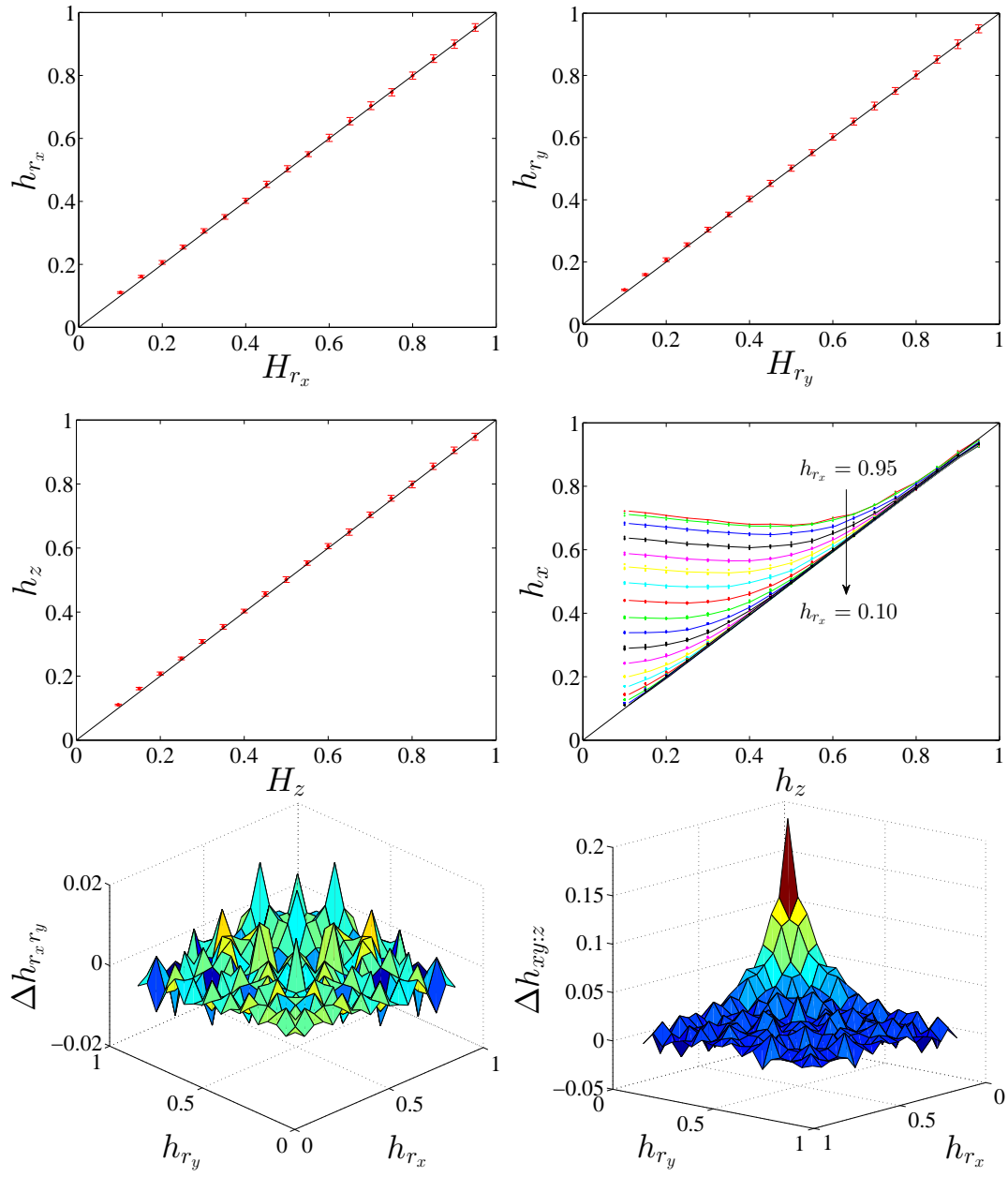


FIG. 5. Comparisons. $\Delta h_{r_x r_y} = h_{r_x r_y} - H_{r_x r_y}$.